Forward and Inverse Modeling of CO_2 and $^{13}CO_2$ in the NCAR CCSM

FINAL REPORT

Scott Denning and Neil Suits
Department of Atmospheric Science
Colorado State University

Peter Thornton
National Center for Atmospheric Research

Background.

The spatial and temporal distribution of CO_2 concentration in the atmosphere contains information regarding sources and sinks at the surface. Quantitative interpretation of this information requires the use of a chemical tracer transport model (CTM) (Enting et al, 1995; Fan *et al*, 1998; Rayner *et al*, 1999; Bousquet *et al*, 2000; Gurney *et al*, 2002). The problem of inverting the tracer transport model to obtain emissions from concentration data is complicated by the fact that regional sources and sinks may produce nearly identical concentration patterns as seen by the present observational network, which cannot be distinguished on the basis of CO_2 concentrations alone. A sink resulting from nitrogen fertilization of the Boreal forest, for example, might produce the same depression in observed CO_2 concentration in the marine boundary layer at 50° N latitude as a somewhat weaker sink resulting from uptake by enhanced phytoplankton productivity in the North Atlantic Ocean. In other words, the matrix relating fluxes and concentrations, which must be inverted to estimate these sinks, is nearly singular

The present research program studies the exchanges of CO_2 and $^{13}CO_2$ between the atmosphere, ocean, and terrestrial biosphere, and the processes that govern them. Spatial and temporal variations of these two tracers in the atmosphere contain information about the sources and sinks of CO_2. The stable isotope ratio $\mathbf{d}^{13}C$ are to be used to reduce uncertainties in regional monthly fluxes calculated by inversion of tracer transport models. The ratio of ^{12}C to ^{13}C fluxes on land depends on physiological stress (which controls isotopic discrimination via stomatal conductance and C_i/C_a ratios) and the pathways and turnover times of photosynthate in ecosystems (which impacts isotopic disequilibrium). We have developed logic describing these processes on land in the Simple Biosphere model (SiB2), which has been successful at predicting variations in CO_2 and $\mathbf{d}^{13}C$ on local, regional, and global scales when coupled to an atmospheric model.

A recent analysis by Randerson *et al* (2002) pointed out that assuming invariant isotopic discrimination might produce systematic bias in deconvolution calculations. The advantage of making this simplifying assumption is that the influence of the terrestrial isotope disequilibrium, i.e. the isotopic difference between assimilated and respired fluxes, is multiplied by the *net* terrestrial CO_2 flux, which is only in the range of 2 to 4 Gt of carbon (Fung *et al* , 1997). If, on the other hand, carbon isotope discrimination changes over time, then subsequent respiration acts on organic matter with the new

isotope ratio and therefore the disequilibrium must be applied to the *gross* respiration flux (typically 20 to 50 times greater!). As a result, a change of *0.2 per mil* in the global isotope discrimination factor can be interpreted as a *0.85 Gt-C* shift in the land versus ocean carbon sink. Of particular interest are the questions of whether interannual variations in discrimination and net assimilation are systematically related, and if they can be correlated with other environmental phenomena, such as El Niño Southern Oscillation (ENSO) or major volcanic activity. If discrimination and primary productivity do covary, then it may be possible to write a linear equation relating discrimination anomalies to productivity anomalies, which would simplify the solution to the inversion problem.

Objectives and Hypotheses

Broadly, the objectives of the proposed research are to develop and test a state-of-the-art coupled simulation model of exchanges of CO_2 and $^{13}CO_2$ in the Earth system, and use it to better quantify sources and sinks of atmospheric CO_2 and understand the processes that control their variability.

Specifically, we identify the following hypotheses:

1. Isotopic discrimination against ^{13}C in terrestrial ecosystems is a function of physiological stress as expressed in stomatal conductance, and can be predicted by tracking ecosystem states (water balance, temperatures) to predict isotopic effects on the atmosphere and the composition of organic matter;
2. The isotopic composition of organic pools in terrestrial ecosystems varies over time in response to the changing atmospheric $\mathbf{d}^{13}C$ and to changes in discrimination; these changes can be used to predict isotopic disequilibrium between land biota and the atmosphere;
3. Spatial and temporal variations in discrimination and disequilibrium can be calculated by a process-based model to estimate their magnitude and uncertainty in such a way that the inverse problem of estimating sources and sinks of CO_2 will be significantly better constrained using $\mathbf{d}^{13}C$ observations than by CO_2 alone.

Methods

The model and isotope simulations.

Meteorlogic data provided by climate models or observations drive the biogeochemical reactions of the Community Land Model (CLM) (Fig. 1). Rates of photosynthesis, respiration and internal plant resistances and CO_2 concentrations are used to calculate photosynthetic carbon isotope fractionation. Fluxes of total carbon and carbon-13 assimilated during photosynthesis are distributed among various organic matter pools and contribute to growth, respiration and changes in concentrations and isotope ratios of canopy CO_2. Ratios of C3 and C4 plants are determined by observation, satellite data or in a dynamic vegetation model.

The terrestrial biosphere can be viewed as single canopy with various sources and sinks for $^{13}CO_2$ and $^{12}CO_2$ (Fig. 2). Canopy CO_2 is assimilated by vegetation during photosynthesis. The ratios of $^{13}CO_2$ and $^{12}CO_2$ fractionated during photosynthesis that imparts a corresponding fractionation on the photosynthate and the canopy air. CO_2 is mixed between the canopy air space and the overlying mixed layer in the atmosphere. This occurs without isotope fractionation. Respired CO_2 is emitted from the soils and reflects the cumulative $\delta^{13}C$ of photosynthate.

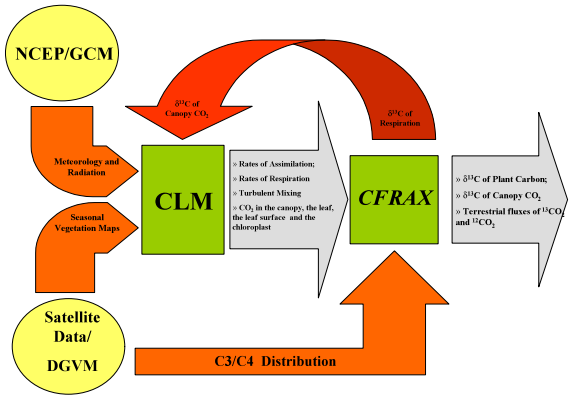

Fig. 1. Flow of data in the simulation. Meteorlogic data are provided by observations (NCEP2) or generated within the CCSM atmospheric model, CAM. Vegetation maps are from processed satellite data or predicted in the CCSM dynamic vegetation model, DVGM. C3/C4 plant distributions are from satellite data and maps of agriculture [Still et al., 2003] or determined by DVGM. CLM calculates 1) rates of assimilation, 2) leaf boundary layer, stomatal and mesophyll conductance, 3) CO_2 concentrations in the plant (C_s, C_i, C_c) and canopy (C_a). The equations in CFRAX, which are now embedded in CLM, calculate carbon isotope discrimination of the photosynthate and canopy air space. $\delta^{13}C$ of respiration is calculated by tracking of decomposition and isotopic fractionation of plant and soil organic pools and therefore provides an explicit estimate of the terrestrial isotope disequilibrium.

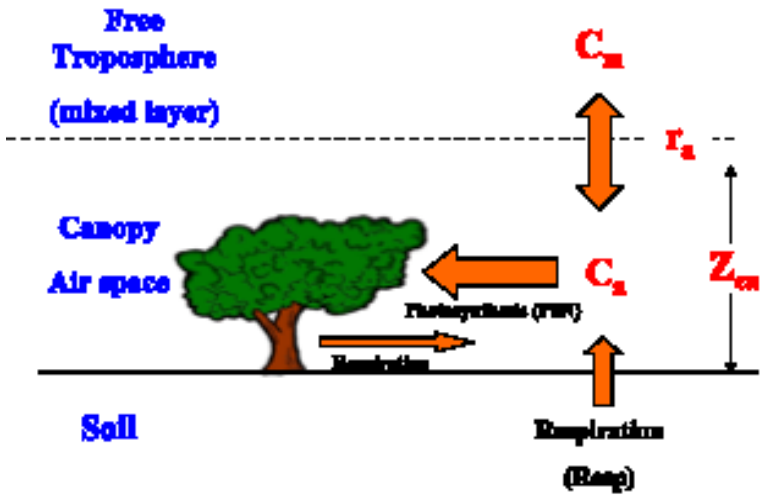

Fig. 2. The terrestrial biosphere. The terrestrial biosphere is broken into three boxes (the overlying atmosphere, the canopy air space and the soil), which exchange CO_2. C_a, C_m are concentrations of CO_2 in the canopy air and mixed layer of the atmosphere, respectively. Arrows indicate the direction of CO_2 flow. R_a is the resistance to exchange between the canopy and the atmosphere. Z_ca is the height of the canopy.

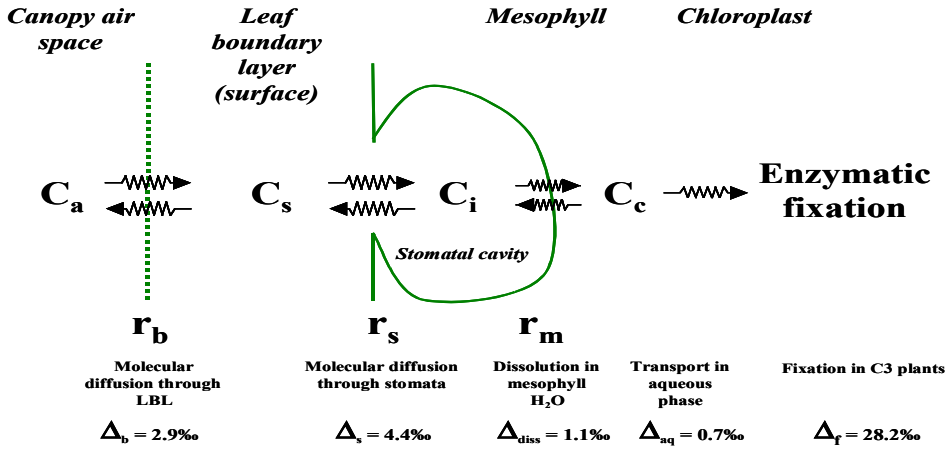

Fig. 3. Representation of carbon flow through C3 plants. C_a, C_s, C_i and C_c are CO_2 partial pressures in the canopy, at the leaf surface, in the stomatal cavity and chloroplast, respectively. r_b, r_s and r_m are resistances to molecular diffusion of CO_2 across the leaf boundary layer, through the stomatal pore and from the stomatal cavity to the chloroplast, respectively. Δ_b, Δ_s, Δ_{diss}, Δ_{aq} and Δ_f are kinetic isotope effects accompanying molecular diffusion of CO_2 across the leaf boundary layer, through the stomatal pore, from the stomatal cavity to the chloroplast (dissolution plus aqueous transport) and enzymatic fixation, respectively [Craig, 1953; Mook et al., 1974; Farquhar, 1983; O'leary, 1984].

Photosynthesis and the accompanying fractionation of carbon isotopes can be viewed as divided into 3 transport steps followed by enzymatic fixation with ribulose

bisphosphate carboxylase/oxygenase (rubisco) (Fig. 3). The net isotope fractionation (equation 1) is a function of the individual concentration drops and the final Cc/Ca ratio.

$$\Delta PS_{C3} = \Delta_b \left(\frac{C_a - C_s}{C_a} \right) + \Delta_s \left(\frac{C_s - C_i}{C_a} \right) + (\Delta_{diss} + \Delta_{aq}) \left(\frac{C_i - C_c}{C_a} \right) + (\Delta_f) \frac{C_c}{C_a}. \quad (1)$$

Results.

Canopy level and plant functional type (PFT) isotope discrimination.

Figure 4 shows the simulated carbon isotope discrimination predicted for 7 different plant function types (PFTs) in CLM. Mid to high latitude C3 plants, (i.e. Boreal Evergreens; WLEF, Wisconsin, broadleaf deciduous; and Oklahoma broadleaf deciduous) show typical C3 diurnal variations in discrimination. Discrimination starts out high due to low rates of net assimilation combined with relaxed stomatal resistances resulting from high relative humidity. As the temperature increases during the day, relative humidity drops and the stomata constrict. This reduces the flow of CO_2 to the chloroplast, resulting in a decline in discrimination. As the temperature drops throughout the late afternoon into the early evening, stomata once again open up allowing the resumption of flow of CO_2 to the chloroplast thus allowing Rubisco to be more 'choosy', i.e., more discriminating, in its selection of CO_2 molecules for enzymatic reactions. The relatively flat diurnal behavior of the tropical (Amazon) broadleaf evergreen pft reflects that corresponding flat variations in daytime weather of the tropical forest. Carbon isotope discrimination of the Oklahoma C4 grass is constant at 4.4‰, as set in the program. C4 plants demonstrate much lower carbon isotope discrimination because of their unique photo-metabolism allows them to survive, and even thrive, in hot dry climates.

Prognostic canopy CO_2 and $\delta^{13}C$ of CO_2.

Prognostic canopy CO_2 and carbon isotope ratios of CO_2 provide us with a method of comparing simulated results to observations taken in the field. The implicit calculations involved are also both more stable and realistic because they give the canopy a true mass and thus a memory of what has occurred in the previous time steps.

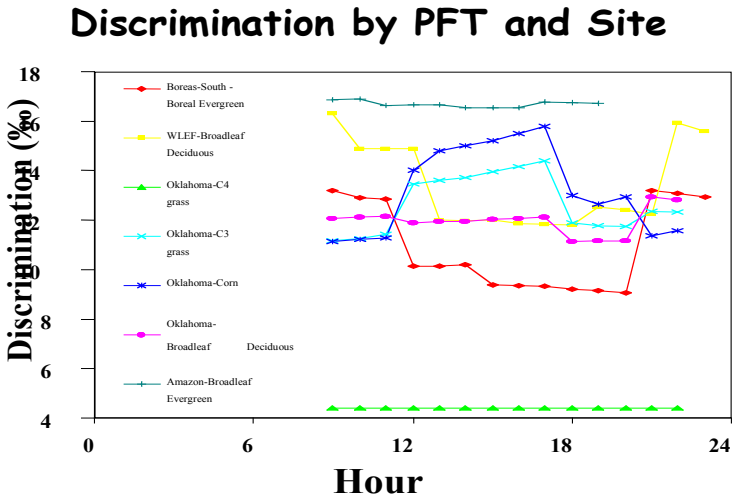

Fig. 4. Simulated diurnal variations in prognostic canopy CO_2 concentrations. Diurnal composites of mean hourly behavior predicted by CLM for the grid cell containing the WLEF tall tower in Wisconsin, U.S.A for 6 different months.

Figure 5a shows simulated diurnal variations in CO_2 concentrations within a grid cell containing the WLEF Tall Tower site in Wisconsin, U.S.A. for every other month of the year. CO_2 concentrations build up during the nighttime because even though photosynthesis has ceased, respiration continues and the nighttime boundary layer is more stable. The magnitude of the concentration build up is a function of the rate of respiration and the degree of atmospheric stability. Generally respiration rates are highest during the summer because the ground is warmer. CO_2 concentrations in the canopy air increase to almost 40 Pa (400 ppmv) in July. This is similar to observations in similar ecosystems (Flanagan et al, 1996). Wintertime CO_2 increases are much lower because even though the boundary layer is generally more stable, the rate of respiration is much, much lower than during the summer. During the day, CO_2 concentrations in the canopy remain relatively close to the concentration of the overlying boundary layer because of high rates of mixing. At times the CO_2 concentrations even fall below the mixed layer concentration because CO_2 is being withdrawn from the canopy air faster than it can be replenished by respiration, or more importantly, mixing with the overlying atmosphere.

Figure 5b shows the accompanying diurnal variations in $\delta^{13}C$ of canopy CO_2 simulated in CLM.. By and large the diurnal behavior of $\delta^{13}C$ of CO_2 is the inverse of the concentrations. Carbon isotope ratios of canopy CO_2 decrease during the night due to an influx of isotopically depleted CO_2 from respiration. This CO_2 is depleted in ^{13}C relative to atmospheric CO_2 because of the discrimination imparted during photosynthesis has been transferred to soil organic matter decomposition pools. $\delta^{13}C$ of the CO_2 returns to the values close to that of the atmospheric boundary layer during the day, largely due to high rates of mixing with the overlying atmosphere. Occasionally, however, $\delta^{13}C$ of the CO_2 becomes enriched relative to that of the mixed layer as a results of a "Rayleigh distillation' effect that preferentially removes $^{12}CO_2$ from the canopy air during

photosynthesis. This effect with impact carbon isotope ratios of photosynthate and is just one of the many non-linear feedbacks in the cycling of carbon and its isotopes by the terrestrial ecosystem.

Spatial controls on discrimination by C3 plants.

Discrimination by C3 plants is largely controlled by relative humidity. During photosynthesis, plants must balance the need for carbon dioxide with the perils of desiccation. Whenever they open their stomata, CO_2 is allowed to enter the leaf. However, at the same time, water is let out. In order to keep the loss of water to a minimum, C3 plants constrict the stomatal pores during times of low relative humidity and open them up again as relative humidity increases. When the stoma are closed the chloroplast cannot be as discriminating in its choice of CO_2 molecules; when they are open, discrimination is at a maximum. This mechanism is the primary cause of variations, both temporal and spatial, in C3 discrimination. Figure 6 shows zonal means of both C3 discrimination and assimilation-weighted relative humidity, where assimilation-weighted relative humidity is photosynthesis multiplied by relative humidity of the canopy air during each time step divided by the total of photosynthesis for the period of interest.

Spatial controls on 'net' discrimination by all (C3 and C4) plants.

Figure 7 shows the map of simulated $\delta^{13}C$ values for C3 plants from CLM. Although the zonal relationship remains, it is also obvious that there is a lot of complexity in longitudinal variations in C3 discrimination that will significantly impact carbon isotope ratios of atmospheric CO_2, and thus on results of inversions using carbon isotopes to infer distributions of global carbon sources and sinks.

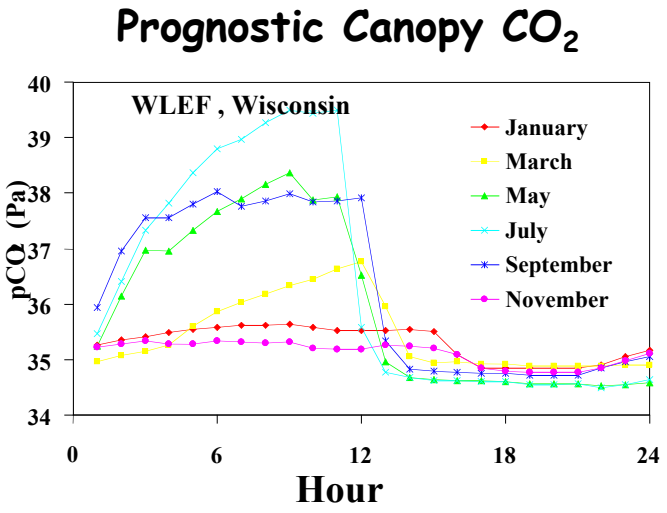

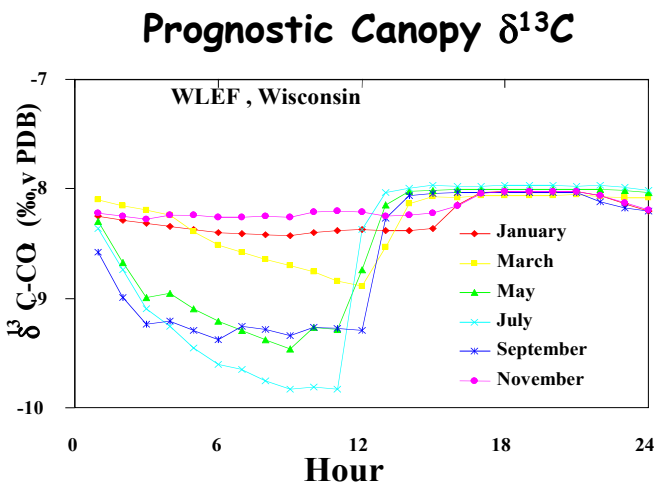

Fig. 5. Simulated diurnal variations in prognostic canopy CO_2 concentrations and carbon isotope ratios. Diurnal composites of mean hourly behavior predicted by CLM for the grid cell containing the WLEF tall tower in Wisconsin, U.S.A for 6 different months.

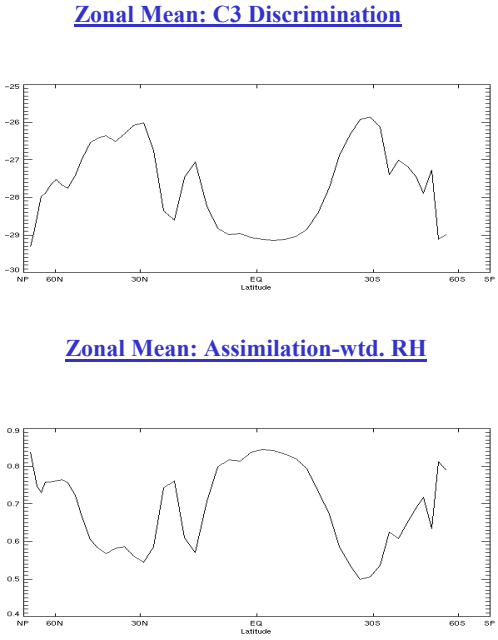

Fig. 6. Zonal means of C3 discrimination and assimilation-weighted relative humidity. Spatial variations in C3 discrimination are controlled by relative humidity. Wet conditions in the high latitudes and tropical forests are reflected in the highly negative $\delta^{13}C$ values of the photosynthate.

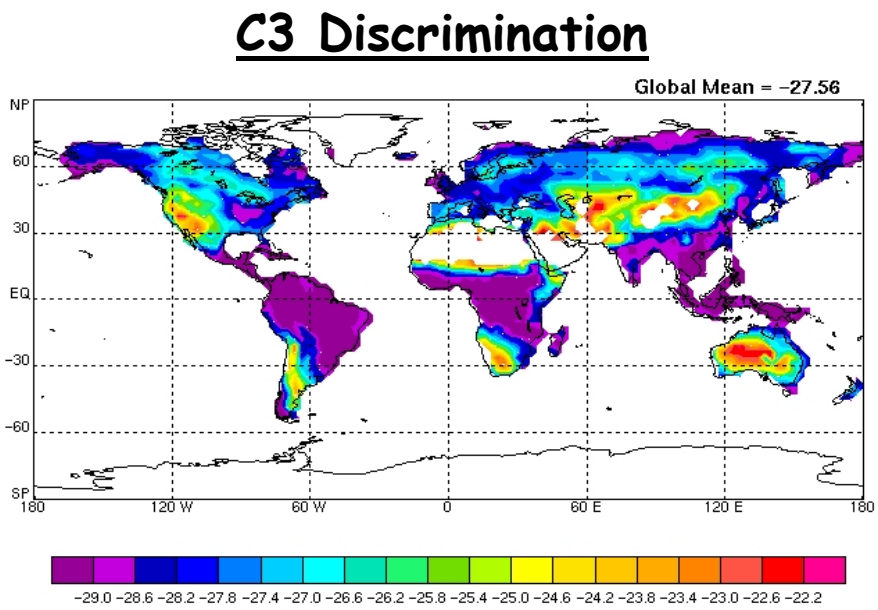

Fig. 7. Map of predicted $\delta^{13}C$ values for C3 plants from a global CLM simulation. The spatial distribution of $\delta^{13}C$ values generally reflects how precipitation and thus relative humidity of the ecosystem.

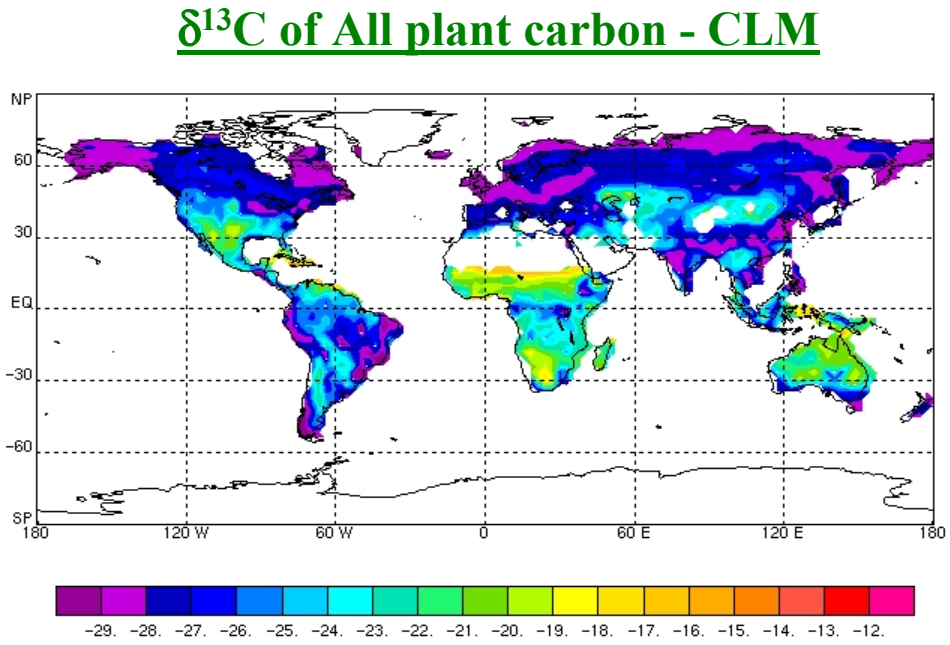

Figure 8. Map of predicted $\delta^{13}C$ values for all plants. This map is constructed from multiyear offline simulations of CLM driven by meteorology provided by the National Center for Environmental Prediction (NOAA-CIRES Climate Diagnostics Center).

Net discrimination is a function of the combined discrimination by both C3 and C4 plants. In CLM, we hold discrimination by C4 plants constant at 4.4‰, the kinetic isotope effect associated with transport of CO_2 through the stomatal pore. Determining 'net' discrimination requires knowledge of the relative proportions of C3 and C4 plant types within a grid cell. SiB2 uses a C4 landmask (Fig. 6) created by Chris Still (Still et al., 2003). The SiB land mask was created using a combination of physiological modeling, satellite observations and knowledge of the distribution of agricultural products. CLM can use the same type of land mask, or generate its own by calculating the distribution of C3 and C4 plants in a dynamic vegetation model. The mask used by CLM in these simulations is an earlier version of the one created by Chris Still. Figure 8 shows the net discrimination of the terrestrial biosphere predicted from CLM simulations averaged over a 12-year period.

What controls temporal changes in discrimination at various spatial scales.

Daily variations in $\delta^{13}C$ of photosynthesis. C3 discrimination changes daily in response to changes vapor pressure deficit (VPD) [Suits et al., 2005]. Using this information we can predict the kind of variations in C3 discrimination that would be expected for a single location. Figure 5 shows mean daily VPD and assimilation-weighted discrimination for the grid cell containing the WLEF tall tower in Wisconsin, U.S.A. The simulated data were taken from the month of August during which time rain had essentially stopped and the system was drying out. Discrimination changes rapidly from one day to the next, but generally reflects the ever-drier conditions in that discrimination declines over the month by approximately 1.5‰. Changes from one day to the next are usually less than 1‰, but occasionally as great as 3‰. As expected, changes in discrimination closely follow corresponding changes in vapor pressure deficit and seem to reflect synoptic scale variability in the weather.

If the predicted changes in discrimination accurately reflect natural variations, we would expect CO_2 uptake to be characterized by low discrimination during dry weather and greater discrimination during wet. Autotrophic respiration reflects this discrimination in root respiration, but it is delayed by between 3 and 10 days, presumably the time that it takes for recent assimilates to be transported from the leaves to the roots and then released as CO_2. Consequently, depending on the time lags involved in synoptic weather variability and plant release of recent assimilates, there could be a very short-lived 'isotope disequilibrium', i.e. the difference in the isotopic ratios of photosynthetic and respiratory fluxes, created in the net ecosystem CO_2 fluxes. These differences are reflected in non-linear variations between the $^{12}CO_2$ and $^{13}CO_2$ net ecosystem fluxes and are an important factor in the use of carbon isotopes provides to double deconvolutions used in inverse modeling. Since most inversions using carbon isotopes look at changes in sources and sinks over interannual and longer timescales, the short-term variations described here will have no impact on those analyses. However, inversions run at shorter time steps and smaller spatial scales could theoretically take advantage of this extra information.

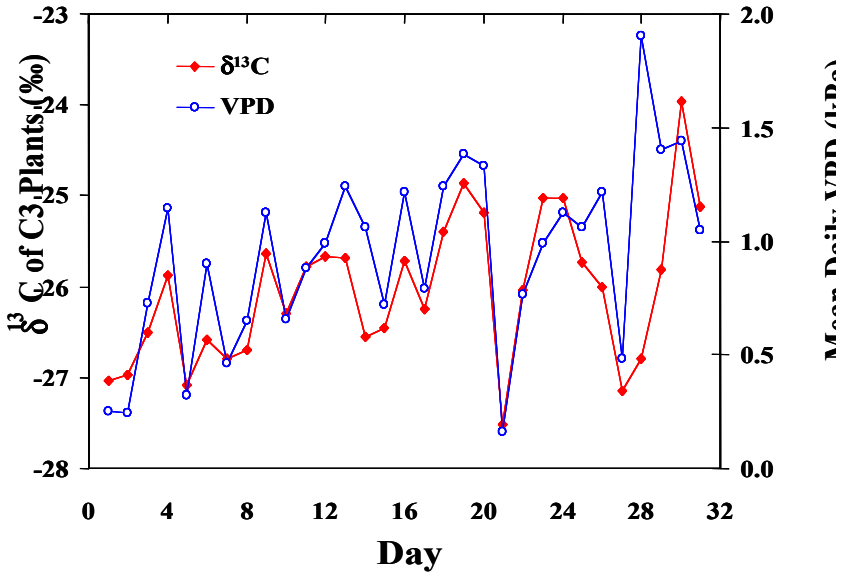

Figure 9. Daily variations in vapor pressure deficit and $\delta^{13}C$ of plant photosynthesis. Large and rapid changes in discrimination reflect synoptic variations in the weather. These variations contribute to a significant short-term isotope disequilibrium.

Statistical correlations

Discrimination and precipitation

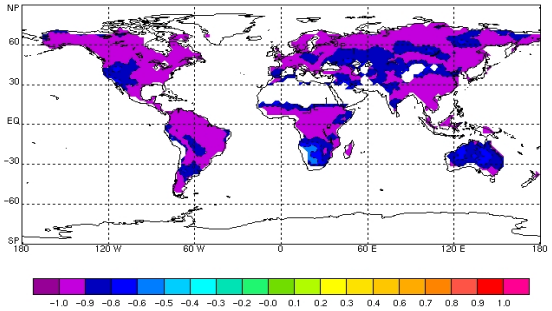

Discrimination and soil water stress

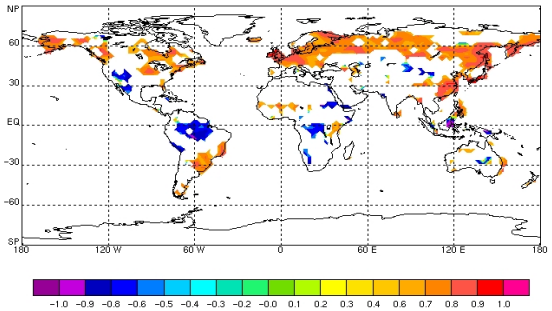

Fig. 10. Statistical correlations between interannual variations in isotope discrimination and precipitation and soil water stress factors. Increased precipitation results in increased discrimination in all biomes. In contrast, increases in soil water stress result in less discrimination in the tropics and increased discrimination in the high latitudes.

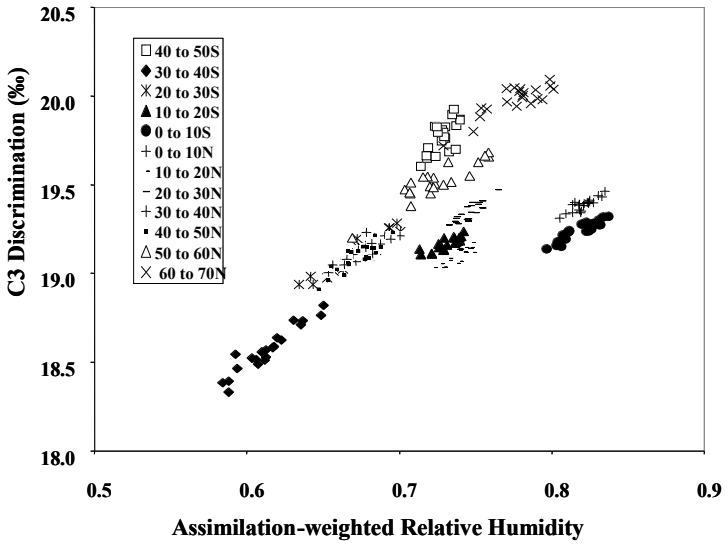

Fig. 11. Zonal relationship between annual C3 discrimination and relative humidity. Discrimination by C3 plants reaches a maximum of 19.0-19.5‰ in tropical forests. At high latitudes, the greatest discrimination occurs during the fall when canopy air relative humidity is high and rates of photosynthesis are depressed.

Interannual variations in $\delta^{13}C$ of photosynthesis. Although the primary control on C3 discrimination is vapor pressure deficit, differences in the seasonal cycles, e.g. air temperature, growing season etc., between the tropics and mid to high latitudes results in a somewhat more complex picture for what controls interannual variations in discrimination. Figure 10 shows statistical correlations at the 1° spatial scale for a linear relationship between annual precipitation, the soil water stress factor and C3 discrimination. For the relationship between precipitation and discrimination the correlation is significant and negative throughout the globe. The carbon isotope ratio is more negative during a wet year, or in other words, C3 discrimination is greater everywhere under wet conditions. In contrast, the correlation between the carbon isotope ratio of photosynthate and the soil water stress factor is negative in the tropics and positive in the mid to high latitudes. The results from several factors, including timing of precipitation in different latitudes, the delay between when it rains and the time it takes for the soil to dry out, the length of the growing season and its impact on early and late season LAI, and the influence of cold temperature on growth rates. While all of these factors contribute to the carbon isotope ratio of the plants, the impact of seasonally cold temperatures is probably the most important in distinguishing high latitude response to those in the tropics.

C3 discrimination is ultimately determined by the balance between rates of photosynthesis and stomatal conductance, and their impact on CO_2 concentrations in the chloroplast [Suits et al. in preparation]. Figure 11 shows zonally averaged annual C3 discrimination as a function of the assimilation-weighted relative humidity. When the

relationship is broken down by latitude band we can see that monthly C3 discrimination reaches a maximum in the tropics of about 19.0 to 19.5 per mil. In contrast, in both northern and southern midlatitudes there are additional temperature considerations that push discrimination to values of 20 per mil and above. The higher discrimination in the mid to high latitudes results from the combined effect of slower growth rates at lower temperatures and higher stomatal conductance due to cool season high relative humidity.

ENSO-induced variations in drought, CO_2 fluxes and isotope discrimination.

Tropical drought can significantly impact inter-annual variations in the terrestrial CO_2 fluxes. Concentrations and carbon isotope ratios of atmospheric CO_2 can help to quantify this impact, however, their use requires a model estimation of the terrestrial isotope disequilibirum, i.e. the difference between the isotopic signature of photosynthesis and respiration, which can only be achieved by accurately accounting for changes in relative contributions of C3 and C4 plants (C4 fraction) and physiological effects of root-zone water stress.

Observations of zonal trends in CO_2 concentrations can be used to infer zonally averaged fluxes from the ocean and atmosphere. Constraints from the isotopic ratios of those fluxes can help to quantify the relative proportions of the fluxes that exchange with the ocean and those that exchange with the terrestrial biosphere. Figure 12 shows zonally averaged CO_2 fluxes for the years 1992 to 2004 [Miller et al. in review]. If we focus on the tropics (17° S to 17°N), we see an enormous net source of CO_2 coincident with the ENSO of 1998-9. Since the total net flux to the atmosphere is well constrained, the isotopes are used to partition the total flux between oceanic and terrestrial sources and thus a large efflux of CO_2 from the land must be balanced by a corresponding decrease in oceanic fluxes. The solid red line in figure 12 is the total CO_2 flux to the atmosphere. The solid green line is the efflux from the terrestrial biosphere assuming that discrimination in the tropics remains constant. However, ENSO are typically associated with drought and that will almost certainly impact the discrimination as well. The dashed and dotted lines on figure 12 give an idea of how these changes in discrimination might affect the estimates of the partitioning of the fluxes. In particular the dashed green line shows that a decrease in discrimination would produce a drop in the estimate of the net terrestrial efflux from approximately 3 GT-C/year to nearly 2 Gt-C/year. So is it reasonable to for there to be a drop in discrimination associated with the 1998 EL Niño, and are there in fact predictable changes in discrimination associated with ENSO?

To examine this question we used a model of the terrestrial biosphere, SiB3, to simulate the magnitude and isotopic signature of CO_2 fluxes between the terrestrial biosphere and the atmosphere for the years 1982-2002. SiB3 is driven globally by 1°X1° NCEP2 assimilated meteorology. Time-varying phenological properties are constrained by processed normalized difference vegetation index (NDVI) calculated from AVHRR.

In the simulation, multiyear declines in re-analyzed precipitation in the tropics preceding the 1982, 1987, 1992 and 1998 el Niños result in spatially complex patterns of both soil water and relative humidity stresses. These, in turn, affect the relative contributions of C3 and C4 plants to total net assimilation, as well as the isotope effect associated with C3 photosynthesis. Variations in the magnitude of C3 discrimination are large; however, because of the lower carbon isotope discrimination associated with C4 plants (~4‰) relative to that of C3 plants (~19‰), relative rates of C3 and C4

photosynthesis are the most important control on discrimination of the terrestrial biosphere. The carbon isotopic signal of each ENSO is unique because each has a spatially unique impact on tropical areas of South America, Africa and Southeast Asia. Changes in tropical net discrimination during the 1998 el Niño are approximately 0.5‰ and are completely driven by changes in the C4 fraction. In contrast, changes in net discrimination during the 1992 el Niño are slightly larger, ~0.6‰, and are driven by variations in both the C4 fraction as well as changes in discrimination by C3 plants.

These results suggest a drop in carbon isotope discrimination could well be typical of the terrestrial biosphere during el Niños, but that systematic relations between CO_2 fluxes and plant discrimination are complicated and controlled by temporal and spatial variations in precipitation, root-zone stress, and their impact on both C3/C4 plant growth, as well as the stomatal response of C3 plants to relative humidity, and therefore we need to look at the specific impact of each ENSO in order to predict its influence on terrestrial discrimination.

A tale of two ENSOs.

1992 ENSO. (Figure 13) Extended drought in tropical South America results in an increase in both relative humidity and root-zone soil water stress, i.e., a decrease in the stress factors. Both C3 and C4 photosynthesis decline, though C3 more so. Increased relative humidity stress causes a decrease in the magnitude of C3 discrimination. At the same time, a relative increase in the contribution of C4 plants to total photosynthesis (C4 Fraction) results in a decrease in the magnitude of Net Discrimination (the combined isotope fractionation of C3 and C4 plants, i.e. e_p).

1998 ENSO. Precipitation rates decline in both South America and Africa just prior to the 1998 ENSO. (Figure 13: Specific tropical regions are not broken out in this figure which shows the integrated values for all of the tropics.) Precipitation continues to decline in Africa in 1998, but has already begun to rebound in South America. Although there is little change in precipitation rates in SE Asia, keep in mind that this only reflects the area between 23°S and 23°N, which excludes a large portion of SE Asian forests. Increases in relative humidity and soil water stress result initially in decreases in C3 photosynthesis. In contrast, C4 photosynthesis actually increases. By 1998, C3 photosynthesis is on the rebound and C4 is now impacted. These independent variations in C3 and C4 photosynthesis produce large variations in the C4 fraction and thus Net discrimination even though there is relatively little change in discrimination by C3 plants.

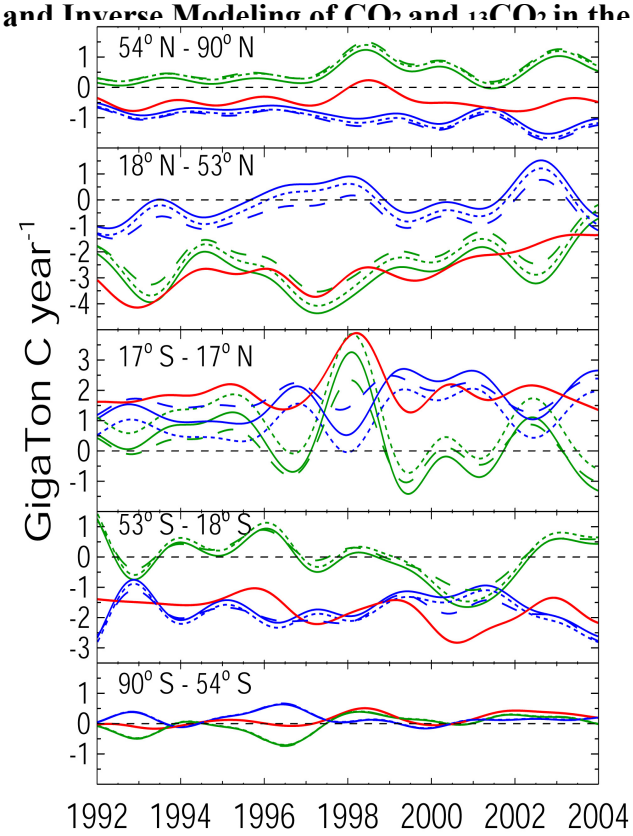

Fig 12. Net zonal CO_2 fluxes. Smoothed monthly surface fluxes (with fossil fuel emissions subtracted) in five zonal bands derived from CO_2 and $\delta^{13}C$ data. The total surface flux (red) is separated into terrestrial (green) and oceanic (blue) components. We test sensitivity of our results to uncertainty in disequilibrium flux and discrimination by varying these terms from our control (solid line). The long dash assumes no C_4 photosynthesis, and **the short dash curves have terrestrial disequilibrium flux doubled**. This shows that the major features of our analysis are robust with respect to our specification of discrimination and disequilibirum. We repeat a single year of output from the model at monthly and 1° x 1° resolution. The inclusion of interannual variability in ε_{ab} and F_{ba} would result in further variability (Miller et al., in review).

ENSO impacts on tropical ^{13}C fluxes

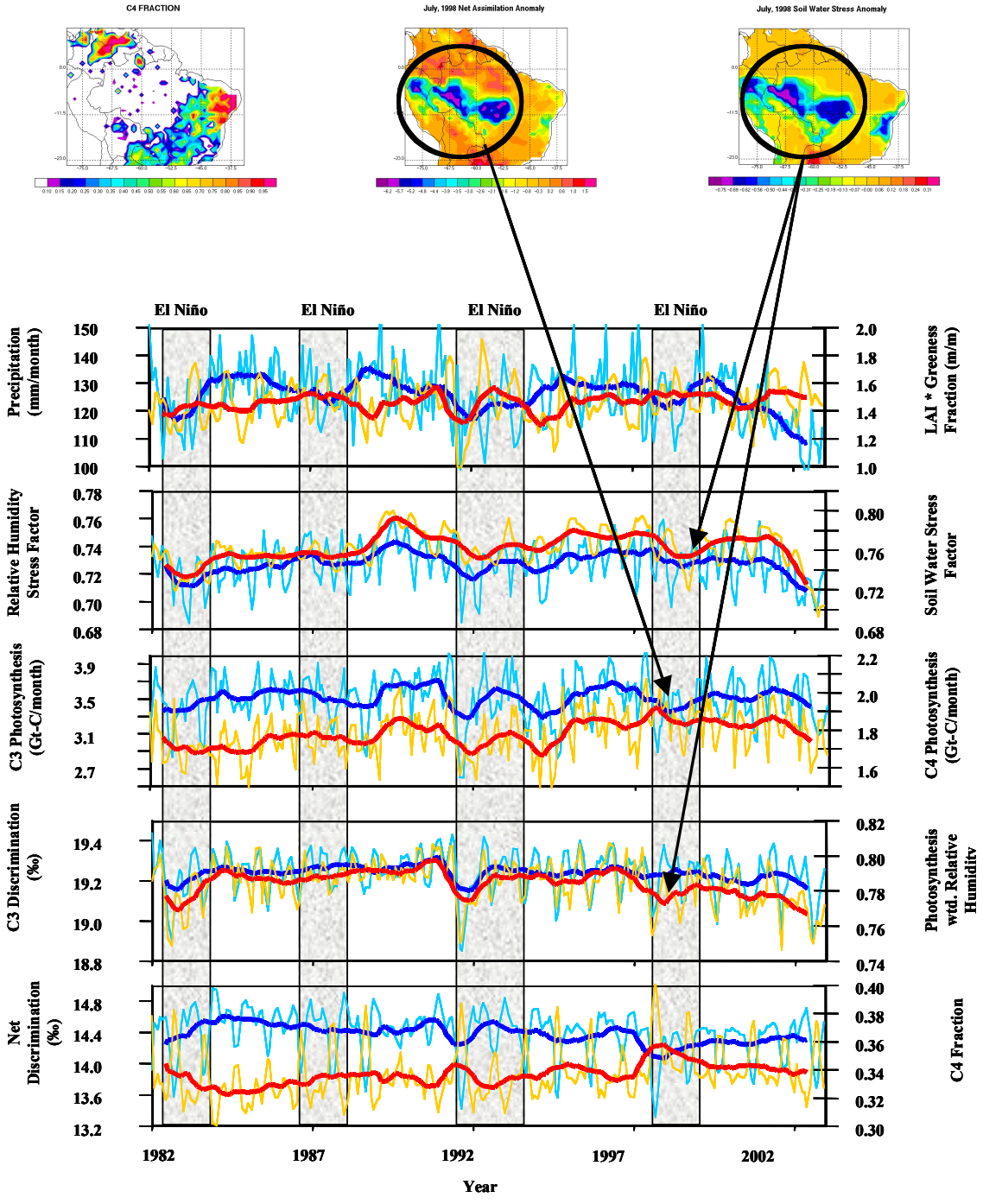

Fig. 13. Modeled variations in precipitation, LAI, RH, soil water and RH stress factors, C3 and C4 assimilation rates, and C3 and Net discrimination for the tropics . The top images are the C4 fraction in the Amazon, the net assimilation anomaly and the water stress anomaly during June, 1998. These anomalies are reflected in the time series of changes in C3 photosynthesis and discrimination, as well a Net discrimination. Note that the response of the terrestrial biosphere to each ENSO is unique.

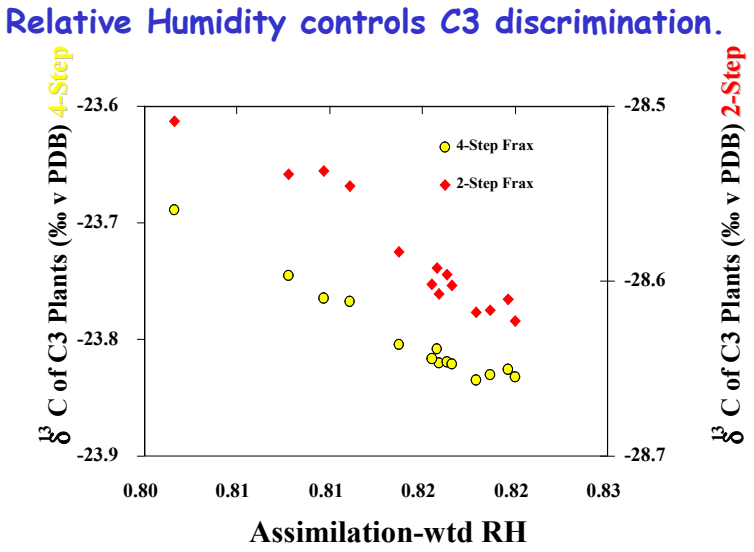

Fig. 14. Relative humidity controls interannual variations in C3 discrimination. There is a strong linear relationship between globally integrated assimilation-weighted relative humidity and the $\delta^{13}C$ of C3 photosynthesis. Discrimination by C3 plants is greater (more negative) at high humidity.

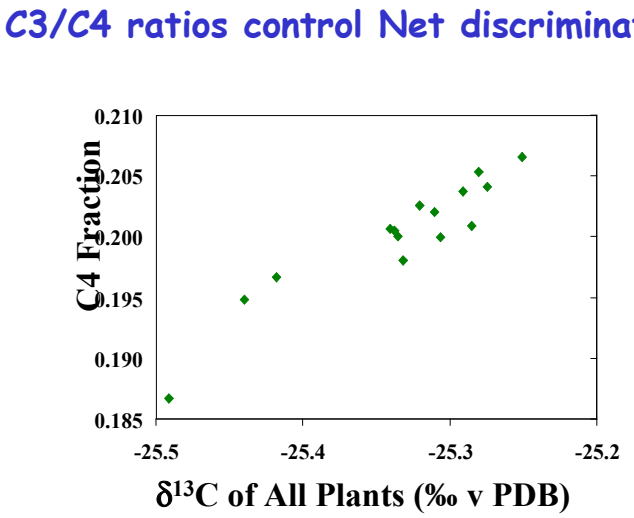

Fig. 15. The relationship between net discrimination and C4 fraction. The dominant control on interannual variations in net discrimination are changes in the relative contributions of C3 and C4 plants.

Controls on globally averaged interannual variations in C3 and net discrimination of the terrestrial biosphere.

Controls on interannual variations in C3 discrimination. Interannual variations in the carbon isotope discrimination by C3 plants at the global spatial scale are controlled by variations in relative humidity. Figure 14 shows a cross plot of annual integrated values of simulated assimilation-weighted relative humidity and $\delta^{13}C$ of photosynthate as simulated in CLM. Results from both two-step and four-step simulations are included. There is a strong linear relationship between C3 discrimination and relative humidity, demonstrating that even at the large spatial scales and long temporal scales, the stomatal response dominates carbon isotope systematics of the terrestrial biosphere. Consequently, we should expect regional droughts, such as those associated with El Niño, to contribute significantly to the global signal in $\delta^{13}C$ of atmospheric CO_2.

Controls on interannual variations in Net discrimination. Figure 15 is a cross plot of the relationship between interannual variations in global net discrimination (the combined carbon isotopic discrimination by both C3 and C4 plants) and the C4 fraction as simulated by CLM. This figure demonstrates that even though C3 plants constitute about 75% of all terrestrial photosynthesis and interannual variations in C3 discrimination can be nearly 0.2‰, that the primary control on interannual variations in net discrimination are changes in the relative contributions of C4 and C3 plants. Changes in the C4 fraction can occur as a result of 1) regional and /or local changes in climate that favor C4 or C3 photosynthetic pathways, and/or 2) regional or global changes in weather that favor C3 ort C4 dominated areas of the terrestrial biosphere. If 'global' or regional warming due to increased CO_2 concentrations in the atmosphere results in warmer, drier conditions, then we might expect a long-term increase in the C4 fraction. On the other hand if increased greenhouse forcing results in warmer, wetter conditions, then C3 plants could be favored. However, an even more likely consequence of increased greenhouse warming is a shift in regional climates, which would then have to be evaluated individually with respect to their impact on C3 versus C4 photo metabolism.

Interannual variations in C3 and net discrimination of the terrestrial biosphere

Figure 16 shows estimates of interannual variations in C3 and net discrimination as well as the primary controls on those changes. The total amplitude of the change in net discrimination in the 21-year period is about 0.3‰. The largest change in net discrimination in a single year is ~0.25‰, or 0.1‰ if we ignore the jump in the first year, which we probably should. The total amplitude of change in C3 discrimination in the 21-year simulation is 0.12‰. The largest single year jump in C3 discrimination is 0.06‰. Changes in net discrimination closely parallel those of C3 Fraction ($R^2 = 0.93$). Changes in C3 discrimination roughly parallel those of Anwtd-RH ($R^2 = 0.60$; for RH: $R^2 = 0.37$). Changes in the first year must be viewed with a grain of salt because we do not know the true initial conditions. We used the conditions at the end of the simulation. However, these conditions resulted in somewhat dry soils in parts of the tropics. Experiments with 'wet starts", i.e., initial conditions after a few wetter than normal years, did not significantly alter the simulated results, however, the fact that C3 assimilation increases in the first year, whereas C4 assimilation decreases suggests that the initial conditions are suspect. By and large increases in C4 assimilation are accompanied by

increases in C3 assimilation. Exceptions to this include the first year and the years 1996-99. There are no clear correlations between ENSO and *global* changes in net discrimination. However, as we have already seen, his is not necessarily true of regional signals such as in the tropics. There is a decline in the C3 fraction throughout most of the simulation. This is generally because of relatively steady C3 assimilation rates accompanied by increases in assimilation rates of C4 plants.

Although there are no clear global responses to all four ENSOs, there are declines in C3 discrimination accompanying the ENSOs of 1992-94 and 1998-99. These changes in discrimination are not restricted to the time period of the ENSO, but are the result of multiyear declines in tropical precipitation and consequent relative humidity. At the zonal spatial scale (Figure 13), responses to ENSO are more pronounced and result from variations in both C3 discrimination and relative changes in C3 and C4 net assimilation rates.

Variability of discrimination at different spatial and temporal scales

Table 1 shows the range of variation in C3 and Net discrimination at various temporal and spatial scales. By and large the range of the variation decreases with increasing spatial and temporal scale. Daily variations at a single site in the mid latitudes (2.5‰) are much greater than those predicted for the tropics (0.9‰). This reflects the greater variability of weather in the mid latitudes from one day to the next. Annual variations at a site also show more variability at higher latitudes (1.1‰) than in the tropics (0.35‰), again reflecting the more constant conditions of the tropical forests. At the zonal spatial scale, monthly variations in discrimination are still slightly greater for the mid to high latitudes compared to the tropics and now we also see slight differences between the northern and southern hemispheres, which reflects the difference in land coverage and distribution of biomes in these two hemispheres. At the global spatial scale, there are still significant monthly variations in C3 (0.6‰) and, in particular, Net discrimination (2.5‰), however, these decrease significantly at the interannual time scale.

Carbon isotope ratios of plant fractions and respiration.

In order to calculate realistic, time-resolved variations in the carbon isotope ratio of respiration and thus accurately predict the magnitude of the terrestrial disequilibrium, it is necessary to track the production and decomposition of all organic carbon within the terrestrial biosphere. This includes not only an accurate estimate of the isotope ratio of the photosynthate, but a realistic depiction of the flow of carbon from its initial assimilation during photosynthesis to its eventual release as respired CO_2. Figure 17 shows estimates of seasonal variations in terrestrial discrimination and the distribution of carbon isotope ratios

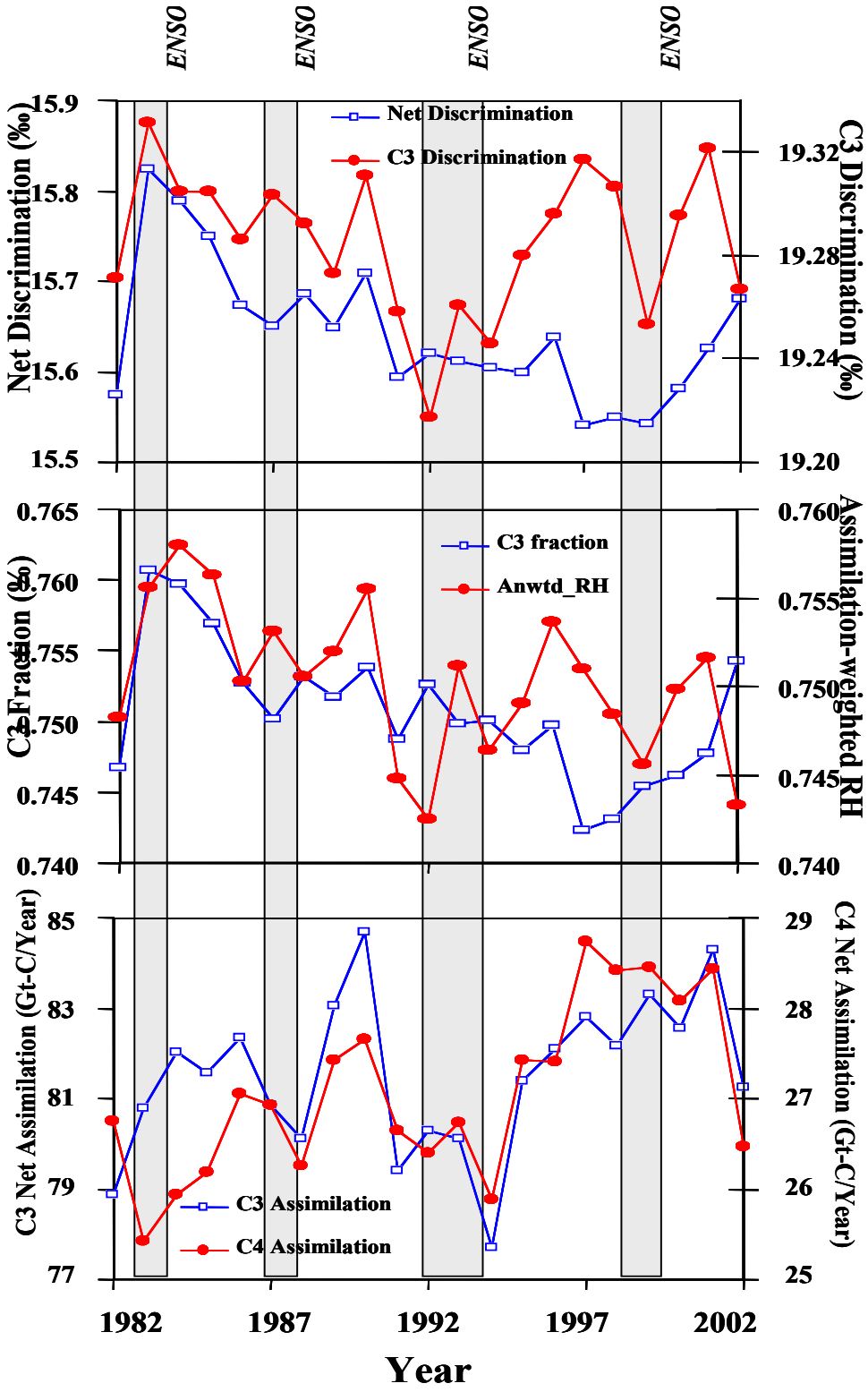

Fig.16 Globally averaged interannual variations in C3discrimination, Net discrimination, the C3 fraction, assimilation-weighted relative humidity, and C3 and C4 assimilation rates. Changes in C3 discrimination track those in assimilation-weighted relative humidity. Changes in Net discrimination track those of the C3 fraction.

Table 1. **Summary of C3 and Net discrimination by temporal and spatial scale**.

	Daily	Monthly	Annual
1° - Midlatitudes (WLEF) (C3 only)	2.5	1.7 (Growing season only)	1.1
1° - Tropics (Santarem) (C3 only)	0.9	2.1	0.35
Zonal – Midlatitudes – (C3)	NA	1.8 (N) 1.6 (S)	0.35
Zonal – Midlatitudes – (Net)	NA	2.1 (N) 2.7 (S)	1.0 (N) 0.6 (S)
Zonal – Tropics – (C3)	NA	1.0 (N) 1.2 (S)	0.13
Zonal – Tropics – (Net)	NA	1.5	0.25 (N) 0.55 (S)
Global – (C3)	NA	0.6	0.12
Global – (Net)	NA	2.5	0.3

Seasonal variations in discrimination

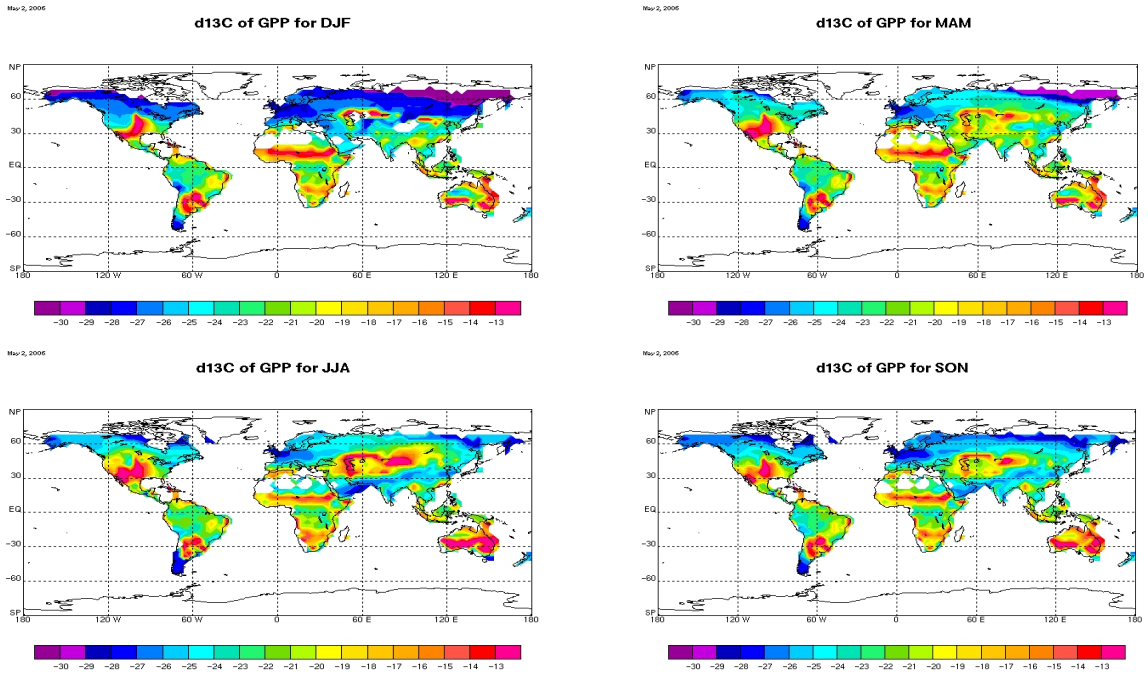

Carbon isotope ratios of 'plant' fractions

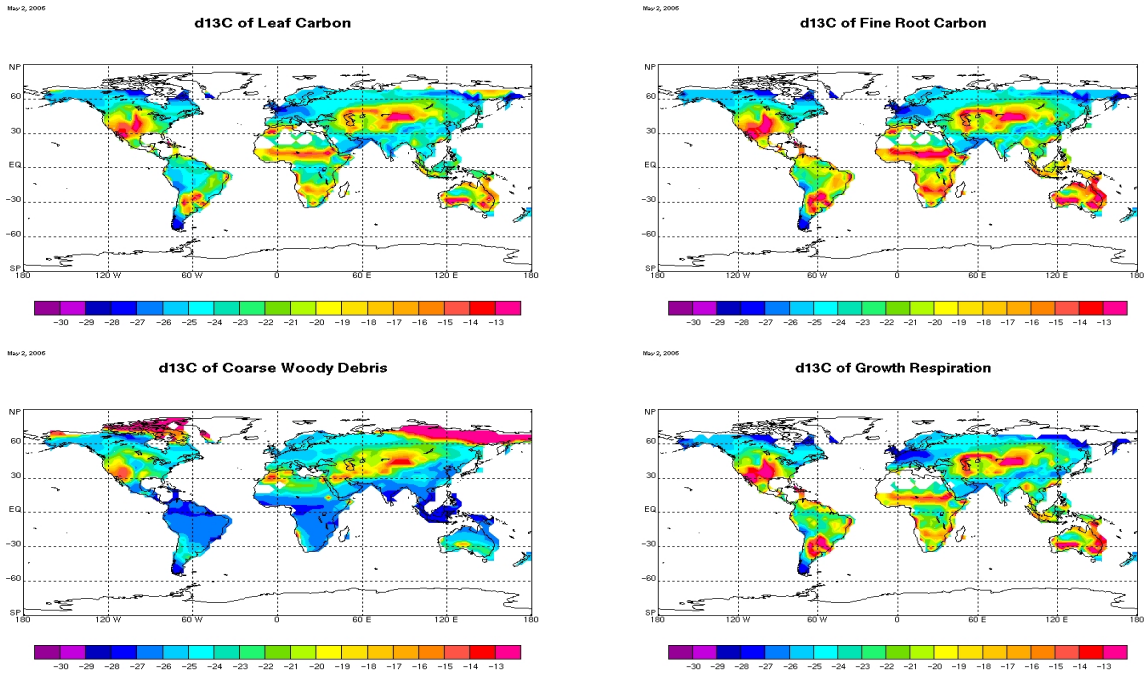

Fig 17. Seasonal variations in isotope discrimination and $\delta^{13}C$ of plant fractions estimated in CCSM.

Summary.

We developed, implemented, and evaluated algorithms for the calculation of biophysical and biochemical fractionation of stable carbon isotopes in the Community Climate System Model (CCSM). Isotopic discrimination during photosynthesis produces fractionated organic matter (e.g., leaves, wood, roots, litter, and soil organic matter). The isotopic composition of the biogeochemical pools in terrestrial ecosystems are tracked as carbon is transferred from one to another over time, and the isotope ratio of ecosystem respiration is calculated as carbon is released to the atmosphere from each of these pools. A prognostic calculation of the CO_2 and its stable isotope ratio in the canopy air space allows photosynthesis fractionate the air from which it draws, and to "recycle" some of the respired carbon. Diurnal cycles and vertical variations of the stable isotope ratio of the air as predicted by the model compare favorably to stable isotope measurements at several sites in the field.

The model was then used to predict global variations of the stable isotope ratio of photosynthesis, respiration, and organic pools worldwide. The strongest spatial patterns reflect the different discrimination by C3 vs C4 plants, but there are important variations over C3 vegetation that reflect physiological stress due to drought and excessive heat. These climate-related variations offer an important new way to evaluate the response of the land module in CCSM to forcing by climate anomalies, and also to use isotope data to better constrain regional fluxes by atmospheric inverse modeling. Variations in the isotope ratio of CO_2 released by ecosystem respiration reflect the turnover time of different storage pools in the ecosystem, and agree well with day-to-day variations observed in several ecosystems. We used the NCEP2 reanalysis climate to drive the isotope fractionation model for an analysis of seasonal and interannual variations in carbon sources and sinks, and stable isotope ratios as they are driven by climate variations. We focused on the response to tropical drought associated with two El Nino events, in 1982-83 and in 1997-98, and showed the impact of climate anomalies on the isotope ratio of atmospheric CO_2 through both changes in the C3/C4 fraction and the stomatal response to relative humidity.

Finally, we performed a 500-year initialization of the terrestrial carbon and isotope pools in CCSM using a prescribed constant isotope ratio for atmospheric CO_2. This allows us to estimate the sizes and isotope ratios of the preindustrial pools. We analyzed seasonal and interannual variability of the fluxes over this period. This run is then used as an initial condition for a 140-year "industrialization" simulation with the atmospheric isotope ratio prescribed according to measurements made on samples from ice cores and from in-situ sampling. We are now preparing a run with the fully-coupled CCSM, given the pools derived by the spinup procedure, and will report results in a subsequent paper.

References cited.

Craig, H., The geochemistry of stable carbon isotopes, *Geochim. Cosmochim. Acta*, 3, 53-92, 1953.

Craig, H., Isotopic standards for carbon and oxygen and correction factors for mass-spectrometric analysis of carbon dioxide, *Geochim. Cosmochim. Acta,* 12, 133-149, 1957.

Bousquet, P, Ciais, P, Peylin, P., Ramonet, M., and P. Monfray, Inverse modeling of annual atmospheric CO_2 sources and sinks. Part 1: method and control inversion, *J. Geophys. Res,* 104, 26,161-26,178, 1999.

Bousquet, P., P. Peylin, P. Ciais, C. Le Quéré, P. Friedlingstein and P. P. Tans, 2000: Regional changes of CO_2 fluxes over land and oceans since 1980. Science, **290**, 1342-1346.

DeFries, R.S., and J. R.G. Townshend, NDVI-derived landcover classifications at global scale, *International Journal of Remote Sensing*, 15, 3567-3586, 1994.

DeFries, R., M. Hansen, J. R. G. Townshend, and R. Sohlberg, Global land cover classifications at 8 km spatial resolution: The use of training data derived from Landsat imagery in decision tree classifiers, *International Journal of Remote Sensing*; 19: 3141-3168, 1998.

DeFries, R.S., Townshend, J.R.G. and M.C. Hansen, Continuous fields of vegetation characteristics at the global scale at 1-km resolution. *J. Geophys. Res.-Atmos*., 104,16911-16923, 1999a.

DeFries, R. Hansen, M., Townshend, J.R.G., Janetos, A.C., Loveland, T.R. A new global 1 km data set of percent tree cover derived from remote sensing. *Global Change Biology*, 6, 247-254, 1999b.

DeFries, R.S., M.C. Hansen. and, Townshend, J.R.G., Global continuous fields of vegetation characteristics: A linear mixture model applied to multiyear 8km AVHRR data. *International Journal of Remote Sensing*, 21, 1389-1414, 2000.

Enting, I.G., C.M. Trudinger, and R.J. Francey. 1995. A synthesis inversion of the concentration and d13C of atmospheric CO_2. *Tellus* **47B**:35-52.

Fan, S., M. Gloor, and J. Mahlman, S. Pacala, J. Sarmiento, T. Takahashi and P. Tans, 1998: A large terrestrial carbon sink in North America implied by atmospheric and oceanic carbon dioxide data and models. Science, **282**, 442-446.

Farquhar, G.D., On the nature of carbon isotope discrimination in C4 species. *Aust. J. Plant Physiol.*, 10, 205-226, 1983.

Flanagan, L.B., J.R. Brooks, G.T. Varney, S.C. Berry, and J.R. Ehleringer. 1996. Carbon isotope discrimination during photosynthesis and the isotope ratio of respired CO_2 in boreal ecosystems. *Global Biogeochemical Cycles* **10**:629-640.

Fung, I., Berry, J. A., Field, C., Thompson, M., Randerson, J., Malmstrom, C., Vitousek, P., Collatz, J., Sellers, P. J., Randall, D. A., Denning, A. S., Badeck, F., and J. John, Carbon-13 exchanges between the atmosphere and biosphere. *Global Biogeochemical Cycles*, 11, 507-533, 1997.

Gurney, K.R., R. M. Law, A. S. Denning, P. J. Rayner, D. Baker, P. Bousquet, L. Bruhwiler, Y.-H. Chen, P. Ciais, S. Fan, I.Y. Fung, M. Gloor, M. Heimann, K. Higuchi, J. John, T. Maki, S. Maksyutov, K. Masarie, P. Peylin, M. Prather, B.C. Pak, J. Randerson, J. Sarmiento, S. Taguchi, T. Takahashi and C.-W. Yuen, 2002: Towards robust regional estimates of CO_2 sources and sinks using atmospheric transport models. *Nature*, **415**, 626-630.

Kalnay, E., and Kanamitsu, M., 1988: Time Schemes for Strongly Nonlinear Damping Equations. *Monthly Weather Review*, **116**(10), 1945-1958.

Mook, W.G., Bommerson, J.G., and W.H. Staverman, Carbon isotope fractionation between dissolved bicarbonate and gaseous carbon dioxide, *Earth Plan. Sci. Let.,* 22, 169-176, 1974.

O'Leary, M.H., Measurement of the isotopic fractionation associated with diffusion of carbon dioxide in aqueous solution*, J. Phys. Chem*., 88, 823-825, 1984.

Randerson, J. T., G. J. Collatz, J. E. Fessenden, A. D. Munoz, C. J. Still, J. A. Berry, I. Y. Fung, N. Suits, and A. S. Denning. A possible global covariance between terrestrial gross primary production and ^{13}C discrimination: Consequences for the atmospheric ^{13}C budget and its response to ENSO. *Global Biogeochemical Cycles*. 2002.

Rayner, P.J., Enting, I.G., Francey, R.J and Langenfelds, R., Reconstructing the recent carbon cycle from atmospheric CO_2, $\delta^{13}C$ and O_2/N_2 observations. *Tellus*, 51B, 213-232. 1999.

Suits, Neil S., A. Scott Denning, J.A. Berry, C.J. Still, J. Kaduk, J.B. Miller and Ian T. Baker, Simulation of carbon isotope discrimination of the terrestrial biosphere. *Global Biogeochemical Cycles*, 19, GB1017, 2005.

Presentations. and papers

Neil S. Suits, A. Scott Denning, J.A. Berry, C.J. Still, J. Kaduk, J.B. Miller and Ian T. Baker, *Simulation of carbon isotope discrimination of the terrestrial biosphere.* Global Biogeochemical Cycles, 19, GB1017, 2005.

Neil S. Suits, A. Scott Denning, Ian T. Baker and Peter E. Thornton. *Challenges to simulating carbon isotopic exchange in the Community Land Model*. 9th Annual Community Climate System Model Workshop, Santa Fe, New Mexico, July 7-9, 2004. (oral presentation to the special meeting on isotopes in CCSM).

Neil S. Suits, A. Scott Denning, Ian T. Baker Gordon Bonan, Peter Thornton, Sam Levis, Keith Oleson and Mariana Vertenstein , *Why we want carbon isotope in CCSM*, Workshop on Isotopes in the Earth System, Boulder, Colorado, January 13-15, 2004. (oral presentation).

Neil S. Suits, A. Scott Denning, Ian T. Baker, Peter E. Thornton and John B. Miller, *Forward and inverse modeling of CO_2 and $^{13}CO_2$ in CCSM*, National Science Foundation, Biocomplexity Awardees Meeting, Washington, D.C., March 12-23, 2004. (poster presentation).

Neil S. Suits, A. Scott Denning, Ian T. Baker and Peter E. Thornton. *Challenges to simulating carbon isotopic exchange in the Community Land Model*. 9th Annual Community Climate System Model Workshop, Santa Fe, New Mexico, July 7-9, 2004. (oral presentation to the special meeting on isotopes in CCSM).

Neil S. Suits, A. Scott Denning, Ian T. Baker Gordon Bonan, Peter Thornton, Sam Levis, Keith Oleson and Mariana Vertenstein , *Why we want carbon isotope in CCSM*, Workshop on Isotopes in the Earth System, Boulder, Colorado, January 13-15, 2004. (oral presentation).

Neil S. Suits, A. Scott Denning, Ian T. Baker, Peter E. Thornton and John B. Miller, *Forward and inverse modeling of CO_2 and $^{13}CO_2$ in CCSM*, National Science Foundation, Biocomplexity Awardees Meeting, Washington, D.C., March 12-23, 2004. (poster presentation).

Miller, J.B., Pieter P. Tans, James W. C. White, Kenneth A. Masarie, Thomas J. Conway, Bruce H. Vaughn, Neil S. Suits, James T. Randerson, *A decreasing trend in Northern Hemisphere carbon uptake since 1992, Science,* in review.

Miller, J.B., James W. C. White, Pieter P. Tans, Kenneth A. Masarie, Bruce W. Vaughn, Thomas J. Conway, Neil S. Suits, James T. Randerson, *Differential environmental controls of terrestrial carbon fluxes in tropical and temperate zones*, in preparation.

Suits, N.S., A.S. Denning, P.E. Thornton, I.T. Baker and J. Lee, *Spatial and temporal variations in terrestrial carbon isotope disequilibria simulated in coupled runs of the Community Climate System Model,* AGU Annual Meeting, San Francisco, CA, December 12-15, 2005, (poster presentation).

Suits, N.S. A.S. Denning, J.B. Miller, *Tropical Drought and the carbon cycle: C3/C4 plant fractions, root-zone stress and the use of carbon isotope discrimination to estimate terrestrial CO_2 fluxes*, Seventh International Carbon Dioxide Conference, Broomfield, Colorado, September 26-30, 2005, (poster presentation).

Suits, N.S., A. Scott Denning, Ian T. Baker, Peter E. Thornton and John B. Miller, *Modeling CO_2 and $^{13}CO_2$ in CCSM*, National Science Foundation, Biocomplexity Awardees Meeting, Washington, D.C., March 21-23, 2005. (poster presentation).

Suits, N.S., A. Scott Denning, Ian T. Baker and Peter E. Thornton. *Simulating carbon isotopic exchange in CCSM*. 10th Annual Community Climate System Model Workshop, Breckenridge, Colorado, July 21-23, 2005. (oral presentation to the special meeting on isotopes in CCSM).

Suits, N.S., A. Scott Denning, Ian T. Baker, and J. A. Berry, *Simulation of carbon isotope discrimination of the terrestrial biosphere on multiple temporal and spatial scales*, in preparation.